25th ABCM International Congress of Mechanical Engineering
October 20-25, 2019, Uberlândia, MG, Brazil

# COB-2019-1343
# ROBUST DESIGN OF ENERGY HARVESTING RESONANT DEVICES BY MULTI-OBJECTIVE OPTIMIZATION

**Paulo H. Martins**
**Marcelo A. Trindade**
São Carlos School of Engineering, University of São Paulo, SP 13566-590, Brazil
paulo.martins@usp.br, trindade@sc.usp.br

***Abstract.*** *The increase in energy consumption in the last decades led to the study of alternative energy sources such as the energy harvested from mechanical vibrations using resonant piezoelectric harvesting devices. The deterministic optimization methods are important to design devices with maximum harvested power. However, uncertainties are present in many mechanical structures and, in this case, non-deterministic optimization is essential for assuring a more robust design, which performance is less sensitive to variations. This work aim to design energy harvesting devices with clamped beams through Sequential Quadratic Programming (SQP) algorithm together with a robust design method known as compromise programming considering uncertainties in devices. This is done using frequency response function (FRF) for power output and squared acceleration input at the clamp and first-order Taylor series approximations for the mean and standard deviation. Results show that optimal and robust energy harvesting devices can be designed accounting for a compromise between harvested power and system's uncertainties following criteria defined by the analyst.*

***Keywords:*** *energy harvesting, piezoelectric materials, optimization, uncertainties, robust design*

## 1. INTRODUCTION

Nowadays, the energy consumption increases considerably and the search for alternative sources has become a necessary research theme. In this context, the energy harvesting concept is interesting because it is related to the conversion of energy into electricity from other energy sources such as mechanical, thermal, chemistry, electromagnetic, etc (Lesieutre *et al.*, 2004). A typical device is composed of piezoelectric cantilever beam with seismic mass attached to its free end and an electric resistor representing a harvesting electric circuit (Franco and Varoto, 2012). The seismic mass is used to tune the device's resonant frequency to the base excitation one. With a piezoelectric sensor bounded to a substrate cantilever beam it is possible to convert the mechanical vibratory energy into electricity (Godoy *et al.*, 2014). The piezoelectric sensors are smart materials with electric dipoles in which electrical charges appear when they are deformed. Figure 1 presents a schematic representation of a typical cantilever beam device used for energy harvesting. With a harmonic displacement $w_0(t)$ at the base it is possible to produce vibration in the device and convert the mechanical energy into electricity. The $m_b$ is the seismic mass used to tune the frequencies, $R_c$ is electric resistor and $l_v$ is the length of the beam.

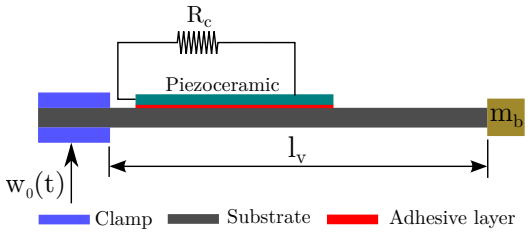


Figure 1. Typical beam used to study on energy harvesting

In order to design well-performing devices optimization methods can be used taking into account the maximum power generated. The deterministic optimization methods aim to find parameters that minimize/maximize a function with certain constraints or conditions. In this work, the Sequential Quadratic Programming (SQP) is used to maximize the power generated and find the optimal devices for this purpose (Rao, 2009). However, if uncertainties in parameters and/or design variables are considered, an uncertainty analysis of the harvested power is essential. In addition, designs without uncertainties are simplifications of the real cases, since changes happen in the environment and the properties of materials, geometry or parameters may have tolerances.

The devices considering uncertainties can be less sensitive to variations in the environment and are known as robust designs. Techniques for robust designs that account for the probability of failure or, alternatively, the sensitivity with respect to changes are known as reliability-based optimization (RBO) and robust design optimization (RDO), respectively (Schuëller and Jensen, 2008). Thus, devices for energy harvesting can be designed through robust design optimization (RDO) in order to produce satisfactory amounts of harvested energy and, at the same time, present low variability considering uncertainties in certain parameters.

Typically, variability decreases in RDO problems whereas the mean value increases such that the analyst must establish the criteria to achieve the best-compromise between mean and variance. In this case, multi-objective optimization can be employed to achieve design variables or parameters that minimize/maximize different functions one at a time. Additionally, the concept of Pareto-front is assumed for the decision making since a set of ideal points is found in multi-objective optimization. In other words, the Pareto-front is a efficient frontier which points are found in convergence criterion and each point can't be changed without compromising other goals (Marler and Arora, 2004). Hence, the analyst can choose subjectively a point in frontier according to a preassigned purpose in project. Thus, a formulation for bi-objective robust optimization (BORD) is presented in this work in order to assure the correct mean-variance trade-off to design beam type piezoelectric energy harvesters with uncertainties in certain parameters. The BORD uses weighting factors for mean and variance functions aim to find a compromise solution based on concept of maximum metric or $L_\infty$ such that this technique in others works is known as Compromise Programming (CP) (Chen *et al.*, 1998). For this purpose, the mean and variance functions can be stated through First-order Taylor approximation ensure the applicability of technique.

## 2. FINITE ELEMENT MODELING OF A PIEZOELECTRIC CANTILEVER BEAM

This work considers an energy harvesting device as shown in Fig. 2 that is composed of a cantilever beam with a piezoelectric sensor, inertial mass $\mathrm{m_b}$ at free end and an electric resistor $\mathrm{R_c}$ connected to the sensor. The imperfect clamping of the harvesting device is simulated using a linear spring $\mathrm{k_w}$ and a torsional spring $\mathrm{k}_\theta$. Figure 2 presents the device with distance from the clamp $\mathrm{d_p}$, piezoceramic thickness $\mathrm{h_p}$, beam thickness $\mathrm{h_v}$, adhesive layer thickness $\mathrm{h_c}$, beam length $\mathrm{l_v}$ and piezoelectric length $\mathrm{l_p}$. Thus, a finite element model is proposed to evaluate the frequency response function (FRF) for power output and harmonic displacement input $\mathrm{w_0}$ based on (Santos, 2008). By means of the theories of Bernoulli-Euler and Timoshenko, the model is proposed taking into account mechanical and electrical degrees of freedom, such that the equations of motion are written as

$$\begin{bmatrix} \mathbf{M}_{rr} & 0 \\ 0 & 0 \end{bmatrix} \begin{Bmatrix} \ddot{\mathbf{u}} \\ \ddot{\mathbf{q}}_c \end{Bmatrix} + \begin{bmatrix} 0 & 0 \\ 0 & \mathbf{R}_c \end{bmatrix} \begin{Bmatrix} \dot{\mathbf{u}} \\ \dot{\mathbf{q}}_c \end{Bmatrix} + \begin{bmatrix} \mathbf{K}_{rr} & -\bar{\mathbf{K}}_{me} \\ -\bar{\mathbf{K}}_{me}^t & \bar{\mathbf{K}}_e \end{bmatrix} \begin{Bmatrix} \mathbf{u} \\ \mathbf{q}_c \end{Bmatrix} = \begin{Bmatrix} \mathbf{F}_p \\ 0 \end{Bmatrix} \tag{1}$$

where $\mathbf{M}_{rr}$ is the mass matrix of system, $\mathbf{R}_c$ the electrical resistance matrix, $\mathbf{K}_{rr}$ the mechanical stiffness matrix, $\bar{\mathbf{K}}_{me}$ the piezoelectric stiffness matrix and $\bar{\mathbf{K}}_e$ the dielectric stiffness matrix. $\mathbf{F}_p$, $\mathbf{q}_c$ and $\mathbf{u}$ are representative vectors for spring force, circuit electric charges and global mechanical displacements, respectively.

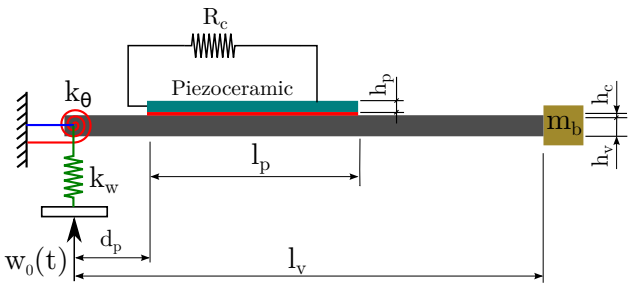


Figure 2. Piezoelectric cantilever beam used as model

Through Eq. (1) the FRF for power output and displacement or squared acceleration input can be found to study the performance (energy harvested) and variability. For this case, the vectors for spring force and global mechanical displacements are stated as $\mathbf{F_p} = \mathbf{b}f_b(t)$ and $\mathbf{u} = \boldsymbol{\phi}\boldsymbol{\alpha}(t)$, respectively. The term $\mathbf{b}$ is a binary column vector in order to ensure the application of harmonic force $f_b(t)$ in correct degree of freedom. Further, $f_b(t) = \tilde{f}_b e^{\omega t}$ with $\tilde{f}_b = k_w w_0$ (i.e., the stiffness coefficient of the linear spring times mechanical displacement at the clamp). The mass-normalized modal matrix $\boldsymbol{\phi}$ is represented in global mechanical displacements and $\boldsymbol{\alpha}(t)$ are the respective modal displacements. Then, for one electric resistor the Eq. (1) may alternatively be stated according to Eq. (2) and Eq. (3) as follows:

$$(-\boldsymbol{\phi}^t \mathbf{M}_{rr} \boldsymbol{\phi}\omega^2 + \boldsymbol{\phi}^t \bar{\mathbf{K}}_{rr} \boldsymbol{\phi})\tilde{\boldsymbol{\alpha}} - \boldsymbol{\phi}^t \bar{\mathbf{K}}_{me} \tilde{q_c} = \boldsymbol{\phi}^t \mathbf{b} \tilde{f}_p \tag{2}$$

$$(j\omega R_c + \bar{K}_e)\tilde{q_c} - \bar{\mathbf{K}}_{me}^t \boldsymbol{\phi}\tilde{\boldsymbol{\alpha}} = 0 \tag{3}$$

In the following steps, the strategy is to assume that $\mathbf{I} = \boldsymbol{\phi}^t\mathbf{M}_{rr}\boldsymbol{\phi}$, $\boldsymbol{\Omega}^2 = \boldsymbol{\phi}^t\mathbf{K}_{rr}\boldsymbol{\phi}$, $\mathbf{K}_p = \boldsymbol{\phi}^t\mathbf{K}_{me}$ and $\boldsymbol{b}_\phi = \boldsymbol{\phi}^t\mathbf{b}$. Thereafter, the matrix for modal damping $\boldsymbol{\Lambda}$ is considered and the Eq. (2) and Eq. (3) are defined as:

$$(-\mathbf{I}\omega^2 + j2\omega\boldsymbol{\Lambda}\boldsymbol{\Omega} + \boldsymbol{\Omega}^2)\tilde{\boldsymbol{\alpha}} - \mathbf{K}_p\tilde{q_c} = \mathbf{b}_\phi\tilde{f}_p \tag{4}$$

$$(j\omega R_c + \bar{K}_e)\tilde{q}_c - \mathbf{K}_p^t\tilde{\alpha} = 0 \tag{5}$$

The circuit current is defined as $I = \tilde{I}e^{j\omega t}$ such that $\tilde{I} = j\omega\tilde{q}_c$. At this stage, the frequency response function (FRF) of circuit current output by displacement at the clamp stated as $G_{Iw}(\omega) = \tilde{I}/\tilde{w}_0$ can be found by calculating $\tilde{\alpha}$ in Eq. (5) and replacing in Eq. (4). Thus $G_{Iw}(\omega)$ is stated as:

$$G_{Iw}(\omega) = j\omega k_w\mathbf{K}_p^t[\mathbf{D}^{-1}]\mathbf{b}_\phi \tag{6}$$

where $[\boldsymbol{D}] = [(j\omega R_c + \bar{K}_e)(-\mathbf{I}\omega^2 + j2\omega\boldsymbol{\Lambda}\boldsymbol{\Omega} + \boldsymbol{\Omega}^2) - \mathbf{K}_p\mathbf{K}_p^t]$. Then, the FRF for power output by displacement at the clamp is defined as $G_{Pw}$ and determined by considering the power as $\tilde{P} = R_c\tilde{I}^2$ and Eq. (6) such that:

$$G_{Pw}(\omega) = R_c G_{Iw}(\omega)^2 \tag{7}$$

Finally, the FRF for power output by square acceleration at the clamp $G_{Pa}$ can be calculated as:

$$G_{Pa}(\omega) = \frac{G_{Pw}(\omega)}{\omega^4} \tag{8}$$

In this work the Eq. (8) is used to investigate the energy harvested through device shown in Fig. 2 and the variance considering uncertainties in certain parameters. This procedure ensures the analysis about performance and robustness for the beam type piezoelectric energy harvester.

## 3. ROBUSTNESS AND MULTI-OBJECTIVE FUNCTION

Uncertainties in variables produce variability in the devices's response. Here, it is assumed that the standard deviation can be used to evaluate this variability. Using a first-order Taylor series approximation, the mean $\mu_f$ and variance $\sigma_f^2$ of an objective function $f(\mathbf{x})$, where $\mathbf{x}$ is a vectors for parameters or design variables, are calculated as (Lee and Park, 2001)

$$\mu_f = f(\mathbf{x}) \tag{9}$$

$$\sigma_f^2 = \sum_{i=1}^{n}\left(\frac{\partial f}{\partial x_i}\right)_\mu^2\sigma_{x_i}^2 \tag{10}$$

where $\mu = [\mu_{x1}, \mu_{x2}, \cdots, \mu_{xn}]^T$. These equations are fundamental for multi-objective and non-deterministic problems, by including both the mean and standard deviation on the design criteria.

Based on the concept of Tchebycheff metric, maximum metric or $L_\infty$ the Compromise Programming (CP) has been addressed in previous investigations for multi-objective functions (Chen *et al.*, 1998). The concept of CP accounts for the following multi-objective problem:

$$\begin{aligned}&\text{Minimize} \quad F(\mathbf{x})\\ &\text{Subject to } \mathbf{x} \in X \subset \mathbb{R}^n\end{aligned} \tag{11}$$

where $X$ is the space of design variables $\mathbf{x}$ and constraints, whereas $F(\mathbf{x})$ is the multi-objective function, in others words $F(\mathbf{x}) = [f_1(\mathbf{x}), f_2(\mathbf{x}), \cdots, f_i(\mathbf{x}), \cdots, f_m(\mathbf{x})]$, with each function $f_i(\mathbf{x})$, $i = 1, 2, \cdots, m$. The minimum value for each function $f_i(\mathbf{x})$ can be described according to the following specifications:

$$\bar{f}_i = \text{minimum}\left\{f_i(\mathbf{x}), \mathbf{x} \in X\right\},\ i = 1, 2, \cdots, m \tag{12}$$

Each minimum value $\bar{f}_i$ leads to a utopia (ideal) point $u_i$ which is defined as:

$$u_i = \bar{f}_i - \epsilon,\ i = 1, 2, \cdots, m \tag{13}$$

where $\epsilon \geq 0$. Hence, a multi-objective optimization problem can be stated based on the concept of the metrics $L_p$, such that:

$$\begin{aligned}&\text{Minimize} \quad \|f(\mathbf{x}) - u\| = (\sum_{i=1}^{m}|f_i(\mathbf{x}) - u_i|^p)^{1/p}\\ &\text{Subject to } \mathbf{x} \in X\end{aligned} \tag{14}$$

where $f(\mathbf{x}) \in \mathbb{R}^m$ and $u \in \mathbb{R}^m$ are vectors formed by elements $f_i(\mathbf{x})$ and $u_i$, respectively, with $i = 1, 2, \cdots, m$. Obviously, the Eq. (14) depends on parameter $p$ which establishes different metrics. The choice for $p = 1$, $p = 2$ and $p = \infty$ lead to Taxicab, Euclidean and Tchebycheff metrics, respectively (Chen *et al.*, 1998). In addition, the problem presented in Eq. (14) can be enhanced by considering weighting factors such that the problem mentioned earlier is stated as:

$$\begin{aligned} &\text{Minimize} \quad (\sum_{i=1}^{m} w_i |f_i(\mathbf{x}) - u_i|^p)^{1/p} \\ &\text{Subject to } \mathbf{x} \in X \end{aligned} \tag{15}$$

where $w_i$ is the positive weighting factor such that $\sum_{i=1}^{m} w_i = 0$. The well-know mathematical expression for weighted sum (WS) method can be found to choose the metric $L_1$ ($p = 1$) in Eq. (15). The WS method is addressed in multi-objective optimization problems because the concepts are readily comprehensible and straightforward. However, for more complicated or non-convex problems the WS method presents weaknesses in relation to the convergence for the global optimum (Lobato, 2008). Additionally, $L_\infty$ metric is used to optimize convex or concave problems and to reach Pareto optimal solution according to weighting factor choose (Moreira, 2015). The CP method is known as weighted Tchebycheff method for $p = \infty$ and employed in this work. Thus, for Tchebycheff metric the optimization is stated as a min-max problem, such that:

$$\min_{\mathbf{x} \in X} \max_{1 \leq i \leq m} w_i (f_i(\mathbf{x}) - u) \tag{16}$$

The problem above can be expressed mathematically as the $\beta$-problem

$$\begin{aligned} &\text{minimize} \quad \beta \\ &\text{subject to} \quad w_i (f_i(\mathbf{x}) + \epsilon - \bar{f}_i) \leq \beta, \quad i = 1, 2, \cdots m. \\ &\mathbf{x} \in X \end{aligned} \tag{17}$$

Here, a similar problem is considered using the mean and standard deviation, as in Eq. (9) and Eq. (10), of harvested power leading to the bi-objective robust design (BORD), such that:

$$\begin{aligned} &\text{minimize} \quad \beta \\ &\text{subject to} \quad w_1 \left( \frac{\mu_f}{\mu_f^\star} + \epsilon_1 - \bar{f}_1 \right) \leq \beta \\ &\qquad\qquad\quad w_2 \left( \frac{\sigma_f}{\sigma_f^\star} + \epsilon_2 - \bar{f}_2 \right) \leq \beta \\ &\qquad\qquad\quad \mathbf{x} \in X \end{aligned} \tag{18}$$

where $\mu_f^\star$ is the ideal (utopia) value for the mean and $\sigma_f^\star$ is the smaller standard deviation obtained by minimizing $\mu_f$ and $\sigma_f$ one at a time, respectively. Through the problem presents in Eq. (18) is possible to verify that the magnitude of constraints is closed because mean and standard deviation are normalized. This considerably simplifies the problem of finding the ideals weighting factors in order to achieve the Pareto-front in convergence process. In despite of this, the analyst need to find minimums values for each function and to optimize the problem for each weighting factor considered.

## 4. ROBUSTNESS OF PIEZOELECTRIC ENERGY HARVESTING DEVICES

The design of piezoelectric energy harvesting devices leads to the optimization process in order to maximize the energy harvested which can be evaluated through Eq.(8). The strategy is to tune the natural frequency of devices and operation frequency to achieve a peak amplitude in FRF for power output by squared acceleration input. Thus, the seismic mass at the free end of the cantilever beam $\mathrm{m_b}$ is used according to Fig. 2 to tune frequencies and electric resistance $\mathrm{R_c}$ employed to calculate the energy harvested. However, a sharp peak amplitude in FRF is verified such that a slight modification in the resonant frequency of devices results in effect of mistuning on the frequency responses and loss of performance. Further, uncertainties in structural parameters may cause variability on the natural frequency of devices decreasing the amplitude of FRF for power output. To assure high performance and low variability the robustness analysis is employed assuming uncertainties in the following parameters of devices: stiffness of the linear and torsional springs, electrical resistance and damping.

In order to design robust energy harvesting devices the seismic mass $\mathrm{m_b}$ and the length of beam $\mathrm{l_v}$ are considered as design variables and electric resistance $\mathrm{R_c}$ is assumed with preassigned value. This allows to establish the following vector

of design variables $\mathbf{x}_p = [\mathrm{m_b}, \mathrm{l_v}]$. On the other hand the uncertain parameters are considered with Gaussian distribution and tolerances of three standard deviations. The function defined in Eq.(8) is posed according to uncertain parameters and design variables such that:

$$f(\mathbf{x}) = G_{Pa}(\omega) = \frac{G_{Pw}(\omega)}{\omega^4} \tag{19}$$

Equation (19) allows to calculate the mean and variance accounts Eq. (9) and Eq. (10), respectively. The mean $\mu_f$ is straightforwardly found considering uncertain parameters in mean values whereas variance is stated as follows:

$$\sigma_f^2 = \left(\frac{\partial f}{\partial k_w}\right)^2 \sigma_{k_w}^2 + \left(\frac{\partial f}{\partial k_\theta}\right)^2 \sigma_{k_\theta}^2 + \left(\frac{\partial f}{\partial R_c}\right)^2 \sigma_{R_c}^2 + \left(\frac{\partial f}{\partial \xi}\right)^2 \sigma_\xi^2 \tag{20}$$

where $\sigma_{k_w}^2$, $\sigma_{k_\theta}^2$, $\sigma_{R_c}^2$ and $\sigma_\xi^2$ are preassigned variance of stiffness of the linear spring, stiffness of the torsional spring, electrical resistance and damping, respectively.

In the next step the CP method is applied to design robust energy harvesting devices based on mean and variance found previously. The problem defined in Eq. (18) requires to find the minimum values for mean and standard deviation (i.e, $\mu_f^\star$ and $\sigma_f^\star$, respectively). Particularly, for the energy harvesting devices mean must be maximized whereas variance or standard deviation minimized. On the other hand, this process implies to find the device with the best performance and other with the lowest variability. Thus, optimization procedures are realized to maximize Eq.(19) and minimize Eq.(20). Consequently, for the vector of design variables lower $\mathbf{x}_p^L$ and upper bounds $\mathbf{x}_p^U$ are established and the SQP method is applied to optimize problems defined in Eq. (21) and Eq. (22) as follows:

$$\begin{aligned} &\text{find} && \mathbf{x}_p \\ &\text{maximizing} && \mu_f \\ &\text{subject to} && f_n = \Omega \\ & && \mathbf{x}_p^L \leq \mathbf{x}_p \leq \mathbf{x}_p^U \end{aligned} \tag{21}$$

$$\begin{aligned} &\text{find} && \mathbf{x}_p \\ &\text{minimizing} && \sigma_f^2 \\ &\text{subject to} && f_n = \Omega \\ & && \mathbf{x}_p^L \leq \mathbf{x}_p \leq \mathbf{x}_p^U \end{aligned} \tag{22}$$

This optimization problems allow to design devices with natural frequencies $f_n$ tuned with the operation frequency $\Omega$ through the equality constraint. This tuning process considers open circuit ($R_c \to \infty$ ) and large magnitude for stiffness coefficients of springs leading to full constraints. On the other hand, the mean and variance are found considering a determined electrical resistance and lower stiffness coefficients $k_w$ and $k_\theta$ ensuring the uncertainties analysis. Hence, the CP method may be applied to design robust energy harvesting devices setting appropriate weighted factors according to the problem defined through Eq. (18) and effects of uncertainties can be verified. Concluding, a complementary statistic analysis through a box plot chart is realized to compare one device with another in relation to the energy harvested.

## 5. RESULTS

For a study case, according to Fig. 2, the parameters, design variables and dimensions are summarized as: distance from the clamp $5\ mm$, piezoelectric thickness $0.25\ mm$, beam thickness $1\ mm$ and adhesive layer thickness $0.1\ mm$, all with width of $25\ mm$ and $l_p = 0.8 l_v$. For the piezoelectric material, the properties are: elastic stiffness constant $\bar{c}_{11}^D = 101.24\ GPa$, piezoelectric constant $\bar{h}_{31} = -1.4862 \times 10^9\ NC^{-1}$, dielectric constant $\bar{\beta}_{33}^\xi = 76.435 \times 10^6\ mF^{-1}$. The Young's modulus and density are $70\ GPa$ and $2700\ kg\ m^{-3}$ for the aluminium beam and $2.5\ GPa$ and $1126\ kg\ m^{-3}$ for adhesive layer, respectively. The modal damping value of $0.3\ \%$ was considered. The base acceleration input has amplitude of $\ddot{\mathrm{w}}_0$ and frequency of $100\ Hz$.

The clamp is simulated with linear and torsional springs with $\mathrm{k}_w = 3000\ kNm^{-1}$ and $\mathrm{k}_\theta = 5\ kNm^{-1}rad^{-1}$, respectively, and tolerance of $50\%$ assigned to each one. The electric resistor and damping are considered with uncertainties such that tolerances are $2\%$ and $10\%$, respectively. Using the FRF for power output by squared acceleration input and compromise programming as in Eq. (18) the problem is formulated considering design variables boundaries. The aim is to find a vector $\mathbf{x}_p = [\mathrm{l}_v, \mathrm{m}_b]$ of design variables such that the problem shown in Eq. (18) is satisfied considering $\mathrm{R}_c = 120k\Omega$. Hence, the SQP method is applied in the energy harvesting problem to find a compromise between mean power $\mu_f$ and standard deviation $\sigma_f$.

In the first stage, the maximum mean power $\mu_f^\star$ and minimum variance $\sigma_f^{\star 2}$ must be achieved trough problems defined in Eq. (21) and Eq. (22), respectively, considering $3\ g \leq \mathrm{m}_b \leq 20\ g$ and $50\ mm \leq \mathrm{l}_v \leq 70\ mm$. Then, the device for

the maximum mean power is found with $\mathrm{l_v} = 50\ mm$ and $\mathrm{m_b} = 13.99\ g$ such that $\mu_f^\star = 94.361\ mWg^{-2}$ whereas for the minimum variance $\mathrm{l_v} = 70\ mm$ and $\mathrm{m_b} = 4.35\ g$ with the result of $\sigma_f^{\star 2} = 2.43\ mWg^{-2}$. The graphs presented in Fig.3a and Fig.3b represent the power generated versus stiffness of linear and torsional springs, respectively, for devices of $\mathrm{l_v} = 50\ mm$ and $\mathrm{l_v} = 70\ mm$. The power generated assumes reasonable variability for $\mathrm{k}_w = 3000\ kNm^{-1}$ and $\mathrm{k}_\theta = 5\ kNm^{-1}rad^{-1}$ in such a manner that these stiffness values were chosen for uncertainties analysis. For higher stiffness values around $\mathrm{k}_w = 15000\ kNm^{-1}$ and $\mathrm{k}_\theta = 8\ kNm^{-1}rad^{-1}$ devices can be tuned because the variability practically vanish enforcing full constraints.

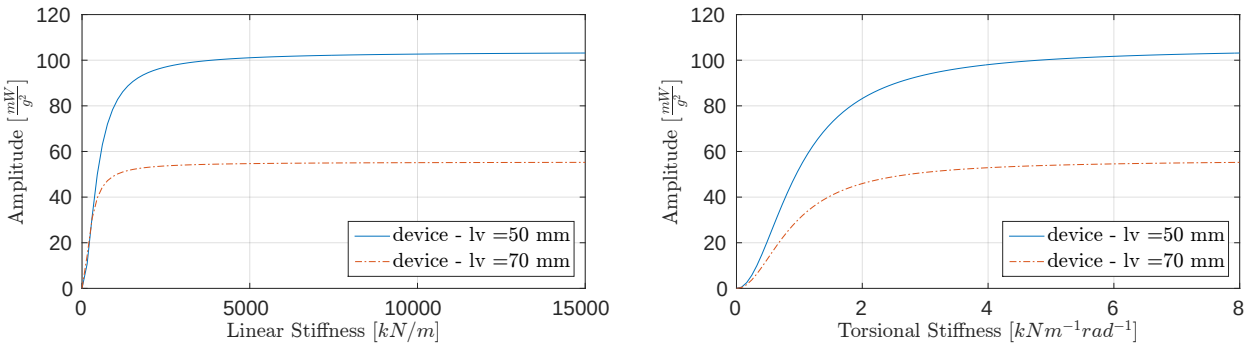


(a) Linear Stiffness

(b) Torsional Stiffness

Figure 3. Power output versus linear and torsion stiffness at the clamp for squared acceleration input

In the second stage, others devices are designed according to the Eq. (18) take into account $\mu_f^\star$ and $\sigma_f^\star$ found previously. The maximum normalized values are $\mu_f/\mu_f^\star = \sigma_f/\sigma_f^\star = 1$ such that $\bar{f}_1 = \bar{f}_2 = 1$. Hence, for $\epsilon_1 = \epsilon_2 = 0$ the utopia point becomes $u^\star = (1;1)$ since $u = \bar{f}_i - \epsilon_i$ and $\bar{f}_1 = \bar{f}_2 = 1$. For certain values of $w_1$ and $w_2$ such that $w_1 + w_2 = 1$ the mean-variance trade-off can be established and devices obtained. Table 1 presents values of design variables, $\mu_f/\mu_f^\star$, $\sigma_f/\sigma_f^\star$ and c.o.v (coefficient of variance) for eleven devices which are found assuming different weighted factors. For $w_1 = 0$ and $w_1 = 1$ the optimization process furnishes design variables similar to those found in converge of problems defined through Eq. (22) and Eq. (21), respectively. Additionally, for $w_1 = 1$ the shorter length device induces better mean power in relation to others cases, but the variance is the largest (c.o.v = 10.27 %). On the other hand, the device with greatest length ($w_1 = 0$) has the smallest values of c.o.v and mean power generated. Choosing weighted factors between $w_1 = 0$ and $w_1 = 1$ with steps of 0.1 others devices are designed through the optimization methodology according to the results presented in Tab. 1.

Table 1. Design variables, mean, standard deviations and c.o.v for different values of $w_1$.

| device | $w_1$ | $\mu_f/\mu_f^\star$ | $\sigma_f/\sigma_f^\star$ | $l_v(mm)$ | $m_b(g)$ | c.o.v (%) |
|---|---|---|---|---|---|---|
| 1 | 0 | 0,566 | 1,000 | 70,0 | 4,35 | 4,56 |
| 2 | 0,1 | 0.593 | 1,093 | 67,5 | 5,05 | 4,76 |
| 3 | 0,2 | 0,614 | 1,137 | 66,4 | 5,40 | 4,77 |
| 4 | 0,3 | 0,622 | 1,199 | 65,3 | 5,73 | 4,97 |
| 5 | 0,4 | 0.641 | 1,279 | 64,0 | 6,09 | 5,15 |
| 6 | 0,5 | 0.656 | 1.339 | 63,1 | 6.50 | 5,27 |
| 7 | 0,6 | 0,681 | 1,455 | 61,7 | 7,08 | 5,51 |
| 8 | 0,7 | 0,724 | 1,677 | 59,5 | 8,04 | 5,98 |
| 9 | 0,8 | 0,776 | 1,985 | 57,1 | 9,18 | 6,60 |
| 10 | 0,9 | 0,854 | 2,533 | 54,3 | 10,84 | 7,65 |
| 11 | 1,0 | 1,000 | 3,982 | 50,0 | 13,99 | 10,27 |

With the results shown in Tab. 1 the Pareto-front is achieved and shown in Fig.4a considering the variance and mean power. The Pareto-front establishes the best solutions or, in other words, a goal or criterion can not be improve without worsening other goal. Thus, the increase in $w_1$ implies smaller devices with higher mean power, but with larger variance such that the device must be chosen according to decision-maker's preferences. In additional, Fig.4b presents the FRF of power output by squared acceleration input for devices designed according to the Tab. 1. For each device the target frequency (100 Hz) is slightly affected due to electrical resistance and uncertainties present in parameters described

previously.

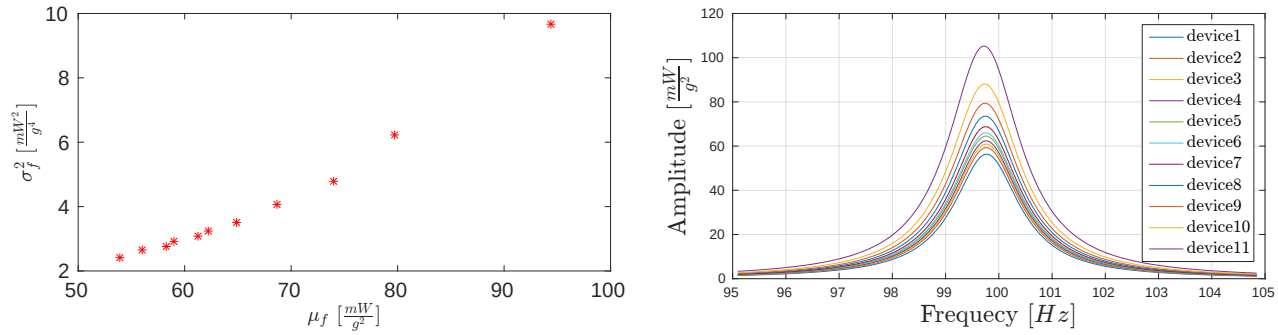


(a) Pareto-front for variance and mean power

(b) FRF for power output by squared acceleration input

Figure 4. Pareto-front and FRF of power output for different devices

Alternatively, a statistic analysis for power generated is realized through the box plot for each device depicts in the Fig. 5. The red line represents the median for power output whereas the bottom and top blue lines the 25th and 75th percentiles, respectively, considering uncertainties in stiffness coefficients, damping and electrical resistance. The upper and bottom limits for whiskers ensure the confidence interval of 99.3% or $+/-2.7\sigma$. Due to the random samples the response presents some points outside the confidence interval, which are represented by red symbol " +" . The Gaussian distribution is assumed in Fig. 5 for devices which are into ascending order. This allows to compare the worst case in relation to the power generated for a determined device with its predecessor. For example, the worst case of power output for device 11 is in the vicinity of 25th percentile for device 10, showing that this last device may reach equal or better performance in relation to its successor for some cases. Additionally, the device 11 is always better than devices 1 to 8 probabilistically although its variability is higher. Thus, a subjective choose may be realized by analyst based on the mean-variance trade-off addressed in CP method and Pareto-front together with statistic analysis through box plots for devices.

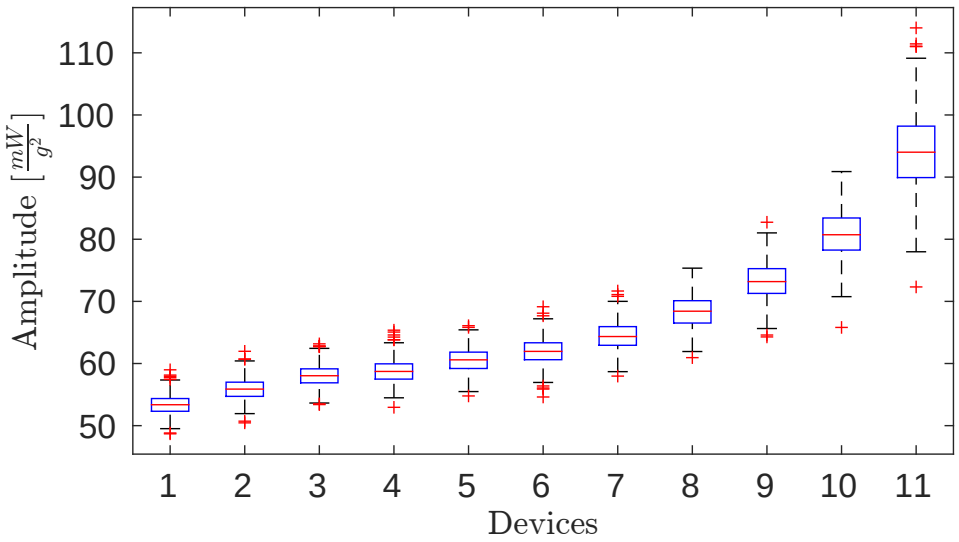


Figure 5. Box plot of power generated for each device considering $+/-2.7\sigma$

## 6. CONCLUSIONS

A study on robust design optimization of piezoelectric resonant energy harvesting devices was presented considering uncertainties in clamping, electric resistor and damping. This was done using a compromise programming technique to maximize mean harvested power and minimize its standard deviation. Both statistical quantities are approximated using first order Taylor series. Results show that devices with larger mass, and thus shorter lengths, lead to better mean performance but also to higher standard deviations. A proper compromise between these parameters can be chosen by the analyst.

## 7. ACKNOWLEDGEMENTS

Financial support of CNPq, grants 574001/2008-5, 309193/2014-1 and 309001/2018-8, and CAPES, through a doctoral scholarship, are acknowledged.

## 8. REFERENCES

Chen, W., Wiecek, M.M. and Zhang, J., 1998. "Quality utility: a compromise programming approach to robust design". *ASME DETC98/DAC5601*.

Franco, V. and Varoto, P., 2012. "Parameter uncertainty and stochastic optimization of cantilever piezoelectric energy harvesters". In *Proceedings of ISMA2012-USD2012*.

Godoy, T., Trindade, M. and Deü, J., 2014. "Topological optimization of piezoelectric energy harvesting devices for improved electromechanical efficiency and frequency range". In *Proceedings of 10th World Congress on Computational Mechanics (WCCM), São Paulo*. pp. 4003–4016.

Lee, K.H. and Park, G.J., 2001. "Robust optimization considering tolerances of design variables". *Computers & Structures*, Vol. 79, No. 1, pp. 77–86.

Lesieutre, G.A., Ottman, G.K. and Hofmann, H.F., 2004. "Damping as a result of piezoelectric energy harvesting". *Journal of Sound and Vibration*, Vol. 269, No. 3-5, pp. 991–1001.

Lobato, F.S., 2008. *Multi-objective Optimization for Engineering System Design (in portuguese)*. Ph.D. thesis, Federal University of Uberlândia.

Marler, R.T. and Arora, J.S., 2004. "Survey of multi-objective optimization methods for engineering". *Structural and multidisciplinary optimization*, Vol. 26, No. 6, pp. 369–395.

Moreira, F.R., 2015. *Robust Optimization Multiobjective for Engineering System Design (in portuguese)*. Ph.D. thesis, Federal University of Uberlândia.

Rao, S.S., 2009. *Engineering optimization: theory and practice*. John Wiley & Sons.

Santos, H., 2008. *Structural vibration control using piezoceramics in extension and shear connected to hybrid active-passive circuits (in portuguese)*. Master's thesis, University of São Paulo.

Schuëller, G.I. and Jensen, H.A., 2008. "Computational methods in optimization considering uncertainties–an overview". *Computer Methods in Applied Mechanics and Engineering*, Vol. 198, pp. 2–13.

## 9. RESPONSIBILITY NOTICE

The authors are the only responsible for the printed material included in this paper.